

1 BEAM-COMMISSIONING STUDY OF HIGH-INTENSITY ACCELERATORS
2 USING VIRTUAL ACCELERATOR MODEL

3

4 H. Harada^{1,*}, K. Shigaki¹, Y. Irie², F. Noda³, H. Hotchi⁴, P.K. Saha⁴, Y. Shobuda⁴, H. Sako⁴, K.
5 Furukawa², S. Machida⁵

6

7 ¹Hiroshima University, 1-3-1 Kagamiyama, Higashi-Hiroshima-shi, Hiroshima 739-8526, Japan

8 ²Accelerator Laboratory, High Energy Accelerator Research Organization (KEK), Tsukuba-shi,
9 Ibaraki 305-0801, Japan

10 ³Energy and Environmental Systems Laboratory, Hitachi, Ltd, 7-2-1 Omika-cho, Hitachi-shi,
11 Ibaraki 319-1221, Japan

12 ⁴Japan Proton Accelerator Research Complex, 2-4 Shirane Shirakata, Tokai-mura, Naka-gun,
13 Ibaraki 319-1195, Japan

14 ⁵Science and Technology Facilities Council, Rutherford Appleton Laboratory, Chilton, Didcot,
15 Oxon OX11, 0QX, UK

16

17 E-mail address: harada@hepl.hiroshima-u.ac.jp (H. Harada*)

18

19

20

21 Abstract

22 In order to control large-scale accelerators efficiently, a control system with a virtual
23 accelerator model was constructed. The virtual accelerator (VA) is an on-line beam simulator
24 provided with a beam monitor scheme. The VA is based upon the Experimental Physics and
25 Industrial Control System (EPICS) and is configured under the EPICS input/output controller
26 (IOC) in parallel with a real accelerator (RA). Thus, the machine operator can access the
27 parameters of the RA through the channel access client and then feed them to the VA, and vice
28 versa. Such a control scheme facilitates developments of the commissioning tools, feasibility
29 study of the proposed accelerator parameters and examination of the measured accelerator data.
30 This paper describes the beam commissioning results and activities by using the VA at the
31 J-PARC 3-GeV rapid-cycling synchrotron (RCS).

32

33 *Keywords:* Virtual Accelerator (VA); Experimental Physics and Industrial Control System
34 (EPICS); Beam Commissioning Tool; High-intensity Accelerator

35

36 1. Introduction

37 Large-scale and high-intensity accelerators typically comprise more than hundreds of devices,
38 and control systems are required to manage all the devices in a unified manner. Such a control
39 system has been constructed by software toolkits and applications based on the Experimental
40 Physics and Industrial Control System (EPICS)[1] and it has given operators easier construction

41 of commissioning tools because operators can identify and control all devices by the record
42 name in the input/output controller (IOC) regardless of the device types. The
43 beam-commissioning tools are constructed for each commissioning stage such as the injection-
44 and extraction-line tuning, a closed-orbit distortion correction, optics correction, and so on.
45 Those tools utilize the functions of the virtual accelerator (VA) [2-4], where the VA is defined as
46 an on-line accelerator model with beam diagnostic devices and is configured under the EPICS
47 IOC for the VA in parallel with the real accelerator (RA). The VA calculates beam
48 characteristics using the RA parameters received from the EPICS IOC as well as any machine
49 parameter set the operator wants to investigate. Parameter sets that the model used can also be
50 available for a RA operation through the EPICS IOC. Each commissioning tool is responsible
51 for the specified VA parameters, such as an optics correction tools for dipole and quadrupole
52 magnet fields with higher-order components, an injection-line tuning tool for injection bump
53 magnet fields, and so on. The VA parameters thus obtained are commonly used by all the
54 commissioning tools. This control scheme with VA enables very efficient beam-commissioning
55 activities. First of all, it greatly facilitates the development of beam-commissioning tools. They
56 can always be debugged and/or tested by running the VA for a virtual commissioning. And, once
57 completed, they are easily converted to those for the RA by changing the suffix of each record
58 name from VA to RA, and consequently the VA greatly decreases the debugging time. Another
59 aspect of this system is, for example, that new magnet parameters for the RA operation can be
60 checked by the VA whether they are acceptable from view point of aperture clearance. If

61 acceptable, the parameters are transferred quickly to the actual RA operation through the IOC.
62 In the beam physics study with the RA, the experimental conditions can clearly be identified
63 beforehand, and the results can also be examined by using the RA.

64 In this paper beam-commissioning results with VA system are reported on a 3-GeV
65 rapid-cycling synchrotron (RCS) of the Japan Proton Accelerator Research Complex
66 (J-PARC)[5]. In the following sections, the outlines of the EPICS and the VA are in section 2,
67 beam commissioning using the VA in section 3, discussions in section 4, and a summary in
68 section 5.

69

70 2. EPICS Control System and the VA

71 2.1 EPICS Control System

72 The EPICS is a set of open-source software tools, libraries, and applications and has been
73 developed collaboratively and used worldwide to create control systems for scientific
74 instruments such as particle accelerators and telescopes and large scientific experiments. Such
75 distributed control systems typically comprise tens or even hundreds of computers. The EPICS
76 uses client/server and publish/subscribe architectures to communicate with various computers.
77 The IOC performs real-world I/O and local control tasks and publishes this information to
78 clients using the channel access (CA) network protocol. An advantage of the EPICS is that the
79 development of tools by physicists is easy because they only need to interface with IOC records
80 for the accelerator devices. By using the channel access client (CA Client), it is possible to

81 read/write (I/O) the set values of the current operation from/to the records in IOCs via a network
82 independent of on the device types.

83 2.2 Construction of VA System

84 A logical accelerator called the VA enables very efficient commissioning and operation of an
85 accelerator. The VA presented here is a beam simulator where a beam monitor scheme is added
86 to an on-line accelerator model and is configured under the EPICS IOC in parallel with a RA.
87 We have constructed a beam-commissioning system based on EPICS IOC including a VA at
88 3-GeV RCS in J-PARC.

89 The beam-commissioning system including the VA is shown in Fig.1. The operation interface
90 (OPI) with a graphical user interface (GUI) and the CA client is used to plot various types of
91 data and to control devices through the IOC. The set value of magnets and the measured beam
92 data in the OPI are stored in the data archive and the data are recalled with the time stamp.

93 The VA is provided with beam diagnostic devices such as a beam position monitor (BPM) to
94 detect the transverse beam position at every turn or the averaged closed orbit, a beam profile
95 monitor to measure the transverse profile in the ring, a beam current monitor to detect the bunch
96 shape, and the beam loss monitor to identify the loss points in the ring. In order to simulate the
97 realistic beam signal with the machine and beam noise, the VA monitor output is added with a
98 fluctuation according to the monitor resolution. As for a precise description of magnets, the
99 measured nonlinear components and interference fields are included in the VA in addition to the
100 measured main component and the effective length of magnetic field.

101 The OPI and VA have been created using SAD[6]. SAD is a computing program that has been
102 developed at KEK since 1986 for designing, simulating, commissioning, and improving an
103 accelerator. Major functions of SAD include structural definitions of beam-lines and
104 components[7], rich matching functions (optics, optical/geometrical, off-momentum,
105 finite-amplitude and spin matching), SAD script programming interface like Mathematica[8]
106 style, 6D full-symplectic particle tracking, Taylor map by automatic differentiation and lie
107 algebraic map for nonlinear analysis with the higher-order nonlinear components up to the
108 normal and skew 42-pole magnetic field component, emittance calculation using 6D
109 beam-matrix method and anomalous emittance calculation[9], a GUI application based on
110 Tkinter (Tcl/Tk)[10] and EPICS CA client capability such as CaWrite, CaRead, and CaMonitor
111 that imply write, read, and subscribe to a record in an IOC, respectively. Additional packages
112 SAD includes are an envelope model calculation and a multi-particle tracking with space charge
113 force.

114 The OPI and VA exchange the information via the IOC. The records with memory space are
115 defined in the IOC and are identified by the record names. For example, the steering magnets
116 are controlled as follows. The records for the kick angles of the steering magnets in the RA and
117 VA are defined as “RA:STM01:ANGLE” and “VA:STM01:ANGLE,” respectively. The kick
118 angle of a steering magnet is transferred from the OPI to the IOC. In the RA, the angle is
119 converted into a current by the measured magnetic field and the current is set into the power
120 supply of the steering magnet. In the VA, the angle is sent to the magnet without conversion.

121 As another usage of the VA, the OPI can directly call the VA as the online model. For example,
122 the initial parameters of the quadrupole magnets for the given betatron tune are calculated by
123 the model and the OPI plots the beta and dispersion functions for the quadrupole strengths.

124 Most of the components in the RA and VA can have communication based on EPICS. However,
125 some of components in the RA are still communicating by the file transfer. These
126 communication paths should be revised in the near future to use the EPICS.

127 3. Beam commissioning by the VA

128 3.1. Betatron Tune

129 A common method to measure the fractional part of betatron tune is to excite transverse beam
130 motion and to detect the transverse beam position over a number of successive turns[11]. The
131 betatron motion is excited by a single kick or white noise. If the beam has momentum spread
132 and the ring has nonzero chromaticity, the betatron oscillations excited by a single kick will
133 quickly fade away. Therefore, an exciter with band-limited white noise is installed in the RCS to
134 excite coherent betatron motion and is then implemented in the VA. The exciter gives the beam
135 a continuous kick by an electric field. The variable parameters of the exciter are the power and
136 frequency range. For a frequency range of Δf_n , the expected value of coherent betatron
137 amplitude is

$$138 \quad x_{rms} \approx \frac{\theta_{rms} \sqrt{\beta_x^e \beta_x^m}}{4} \frac{f_0}{\sqrt{\pi \Delta f_n \Delta f_b}}$$

139 where θ_{rms} is the rms kick-angle; β_x^e , the beta function at the exciter; β_x^m , the beta function at

140 the monitor; f_0 , the revolution frequency; and Δf_b , the rms value of the betatron tune spread[12].

141 The kick angle is given by

142
$$\theta_{rms} \approx \frac{eL}{pc} \left(1 + \frac{1}{\beta} \right) \frac{\sqrt{ZP}}{d}$$

143 where L is the electrode length; p , the momentum; e , the electron charge; β , the Lorenz factor;
144 c , the speed of light; Z , the impedance of the deflector electrode; P , the output power of the
145 exciter amplifier; and d , the distance between electrodes.

146 The BPM for tune measurement is installed in the nondispersive section of the ring and detects
147 the transverse beam oscillation. The detected signal is analyzed by a discrete Fourier transform
148 (DFT) package. The exciter parameters are adjusted so that the betatron tunes can be identified
149 as the highest sideband peak of the revolution frequency.

150 The beam condition and the exciter's parameters for the tune measurement are examined by
151 the VA. The simulation is the multi-turn and multi-particle tracking with the exciter on and
152 without chromatic correction. The BPM outputs the beam position turn by turn and the
153 fractional part of the tune is directly obtained from the DFT spectrum. As mentioned previously,
154 a noise fluctuation of 0.5 mm is added to the VA BPM position, according to an assumed
155 monitor resolution. When the resolution is poorer, the pedestal of the DFT spectrum is higher.
156 However, the pedestal can be lowered by averaging the BPM signals over an appropriate
157 number of cycles. The chopped beam from the LINAC is captured in the RF bucket and the
158 chopping factor is defined as the ratio of the chopped beam length to the RF bucket width and is

159 equal to 0.56 in the normal condition. With the maximum output power of the exciter, 1 kW, we
160 could not detect the tune peak of the beam in the normal chopping condition and without
161 chromaticity corrections. We have found that the chopping factor should be less than 0.07 in
162 order to clearly identify the tune peak in case of no chromatic correction. With chromatic
163 correction, the factor of 0.11 is adequate for the measurement and the spectrum is shown in
164 Fig.2. These consequences are taken into account in the tune measurements procedure with the
165 RA.

166 We constructed an OPI for the tune measurement. The turn-by-turn beam oscillation was
167 detected as the difference of the two BPM electrodes without beam current normalization. In the
168 RCS, the revolution frequency and sampling rate are 469 kHz and 6.4 MHz, respectively. The
169 betatron tune peak is identified as the upper and lower sidebands of the revolution frequency
170 peak as shown in Fig. 3, where the chromaticity is corrected and the chopping factor is 0.11.
171 From the spectrum, the betatron tune was derived to be 6.300 ± 0.002 . Good agreement is
172 obtained with the VA results in Fig. 2.

173 3.2. Chromaticity

174 The chromaticity ξ is defined by $\Delta\nu/(\Delta p/p)$, where $\Delta\nu$ is the betatron tune difference; Δp , the
175 momentum difference; and p , the synchronous momentum.

176 The betatron tune is measured vs. beam momentum, where the momentum shift is created
177 changing the RF frequency adiabatically. The chromaticity is then derived from the slope of the
178 betatron tune with respect to its momentum. A frequency shift Δf changes the beam momentum

179 by an amount

$$\frac{\Delta f}{f} = \eta \frac{\Delta p}{p}$$
$$\eta = -\left(\alpha - \frac{1}{\gamma^2}\right)$$

181 where η is the slippage factor; α , the momentum compaction factor; γ , the Lorenz factor; and f ,
182 the RF frequency for the synchronous particle.

183 We have virtually measured the betatron tune by changing $\Delta f/f$ from -0.00414 to 0.00414 in
184 steps of 0.00207 in the beam storage mode. The RF frequency was changed adiabatically during
185 the period from 2 to 10 ms after injection so that the particles do not dilute within the RF bucket,
186 and a large portion of particles concentrate near the synchronous angle. Under these conditions,
187 a betatron sideband peak can easily be obtained with the chopping factor of 0.07 as described in
188 Section 3.1. The $\Delta f/f$ versus horizontal tune ν_x is shown in Fig.4. With the calculated slippage
189 factor, the horizontal and vertical chromaticities were -9.78 ± 0.14 and -6.89 ± 0.14 ,
190 respectively. The error is due to the DFT resolution and the error of least square fitting. The
191 results agree well with analytical calculations of $\xi_x = -9.80$ and $\xi_y = -6.92$. In the virtual
192 measurements and analytical calculations, higher-order magnetic components were essential to
193 produce such values. The typical cpu time for one betatron tune measurement by the VA is about
194 two hours with 10000 particles.

195 Based upon the good agreement, the same procedure was applied to the measurements in the
196 RA. After the optics corrections described in Section 3.5, the chromaticities were obtained to be

197 -9.80 ± 0.14 and -7.03 ± 0.71 for the horizontal and vertical directions, respectively. The $\Delta f/f$
198 versus horizontal tune ν_x in the RA is also shown in Fig.4. The errors are estimated from the
199 DFT resolution and the error of least-square fitting.

200 3.3. Commissioning tool for injection line

201 The RCS injection adopts the H^- injection scheme and 235 turns of H^- beams are injected into
202 the RCS during 500 μsec . In the horizontal plane, the scheme consists of 2 septum magnets
203 (ISEP1, 2) in the injection line, 2 septum magnets (DSEP1, 2) in the dump line, 4 shift
204 bump-magnets (SB1-4) for fixed orbit bump, and 4 paint bump-magnets (PB1-4) for
205 time-varying orbit bump. In the vertical plane, 2 paint magnets (VPB1, 2) are installed in the
206 injection line for painting injection to directly control the injection angle at the stripping foil[13].
207 The system is shown in Fig.5. The SBs that are installed in a drift space between the focusing
208 magnet(QFL) and defocusing one(QDL) has a split-type structure for installation of the
209 stripping foils, and they are excited in series by a single power supply. The incoming H^- beam is
210 almost stripped to H^+ , and is injected into the ring. The unstripped beams (H^0 and H^-) are finally
211 stripped to H^+ at the downstream 2nd and 3rd foils. In the figure, MWPM stands for multi-wire
212 profile monitor, which detects the beam shape and position.

213 The SBs with a large aperture are closely installed between quadrupole magnets (QFL and
214 QDL). Consequently, the measured field of these magnets causes interference, as shown in Fig.6.
215 Field measurements have been performed separately for magnet pairs such as two shift-bumps
216 and a pair of shift bump and quadrupole magnet. The results were then joined together to

217 produce the whole field from QFL to QDL in the figure. The injected beam passes through a far
 218 side of the magnet apertures, where the nonlinear fields may cause some betatron resonances
 219 during the injection period. The measured field in Fig. 6 is divided into 20mm segments along
 220 the beam direction. The magnetic field in each segment was expanded by a Taylor series up to
 221 decapole component, and is incorporated into the VA line as a magnet with a 20mm effective
 222 length.

223 We have constructed a commissioning tool for beam injection. The injection line ISEPs are
 224 controlled as follows. A response matrix “A” is obtained as $\Delta x_i = \sum A_{ij} \Delta \theta_j$, where Δx_i is the
 225 beam deviation at the i-th MWPM; $\Delta \theta_j$, the kick angle by the j-th ISEP; and

$$226 \quad A = \begin{pmatrix} \frac{\partial x_3}{\partial \theta_1} & \frac{\partial x_3}{\partial \theta_2} \\ \frac{\partial x_4}{\partial \theta_1} & \frac{\partial x_4}{\partial \theta_2} \\ \frac{\partial x_5}{\partial \theta_1} & \frac{\partial x_5}{\partial \theta_2} \end{pmatrix}.$$

227 Further, the deviations at the MWPMs are related to beam position and angle at the 1st foil as

$$228 \quad \begin{pmatrix} \Delta x_3 \\ \Delta x_4 \\ \Delta x_5 \end{pmatrix} = \begin{pmatrix} 1 & -L_3 \\ 1 & -L_4 \\ 1 & +L_5 \end{pmatrix} \begin{pmatrix} \Delta x_f \\ \Delta x'_f \end{pmatrix}$$

229 where L_i is the length of the i-th MWPM from the 1st foil.

230 Using these equations and the position measurements at the MWPMs, the beam positions along
 231 the injection line should be adjusted to the design values, while the dump line DSEP settings are
 232 tuned by these equations using position measurements at the MWPMs located in the line. In the
 233 first commissioning, the response matrix obtained by the VA could control the beam positions to

234 the designed ones at MWPMs with a few iterations. After this procedure, the response matrix
235 was measured by the RA, resulting in the precise control of the positions without the iteration.
236 Since the VA has the same control procedure as the RA, the transition from the VA to the RA is
237 done by only changing the selection of the record name and is very smooth. This function
238 facilitates the painting injection studies[14].

239 3.4. BPM polarity

240 In the RCS, 54 BPMs are installed for the measurement of closed-orbit distortion (COD). The
241 measured COD is corrected by 26 steering magnets. In the first commissioning, it is essential to
242 check whether BPM's data are right or not. The displacements (Δx , Δy) of all BPMs were
243 measured for kicks by some steering magnets in the RA and were compared with those in the
244 VA. The sign of displacements was inconsistent for 18 BPMs, which implied the cable
245 connections of these BPMs were reversed. Then, the polarities of these BPMs were corrected in
246 the data processing stage hereafter. The beam-based alignment of the BPM will be performed in
247 the future.

248 3.5 Optics Correction

249 Sixty quadrupole magnets are installed in the RCS and are grouped into 7 families. Although the
250 currents for the required quadrupole strength are calculated by using the measured field data, some
251 errors are unavoidable in the actual current setting.

252 The beta function was estimated from the response of COD for a kick by the steering magnets. The
253 dispersion function was estimated similarly for a momentum shift by the RF. The differences

254 between the designed and measured optics parameters are clearly seen in Fig.7. Then, the VA
255 calculated the strength of the quadrupole magnets to reproduce all of these measurements and
256 betatron tune which was independently measured. The difference of the set and calculated values,
257 which are called “fudge factor,” are stored as a correction factor in the VA. The fudge factors are
258 several percent in the RCS. The optics parameters with corrected current setting agree very well with
259 the measurements as shown in Fig.8. Presently, different fudge factors should be obtained when we
260 largely move on to the different operation point.

261 4. Discussion

262 In high-intensity accelerators, it is necessary to determine the beam loss with good accuracy. In
263 order to examine whether the beam and machine parameters fulfill the required conditions,
264 multi-particle tracking simulations with space charge force are highly required. Further, in
265 determining the extraction orbit, it is very important to know how the beam halo extends,
266 because an aperture of the extraction channel is limited and it may cause some beam losses
267 unless the beam orbit is precisely controlled by taking into account the beam halo distributions.
268 However, the space-charge calculations for a complete acceleration cycle would take several
269 weeks with more than 2×10^5 particles. Although attempts have been made to reduce the CPU
270 time by using parallel computers, we are still far from incorporating the calculations into the
271 online model of the VA. The space-charge calculations are now being performed in an offline
272 system in the RCS.

273 5. Summary

274 A VA system based on the EPICS was constructed and used in the beam commissioning of the
275 3-GeV rapid-cycling synchrotron (RCS) at the J-PARC. The VA is configured under an EPICS
276 server called the input/output controller in parallel with the real accelerator (RA). Since the VA
277 is provided with a beam diagnostic system, a virtual run is possible for developing various types
278 of commissioning tools. During beam commissioning in the RA , examination of the measured
279 accelerator data as well as calculation of the correction factors have also been performed very
280 efficiently.

281

282 *Acknowledgment*

283 The authors would like to express their sincere thanks to all of the RCS staff who worked
284 tirelessly for successful beam commissioning. One of the authors (H. H.) is grateful to Prof.
285 Katsunobu Oide for his kind suggestions and comments during the course of this research.

286

287 *References*

288 [1] EPICS home page, <<http://www.aps.anl.gov/epics>>.

289 [2] N. Yamamoto, Use of a virtual accelerator for a development of an accelerator control
290 system, in: Proceedings of 17th IEEE Particle Accelerator Conference (PAC97), Vancouver,
291 British Columbia, Canada, 12–16 May 1997, p. 2455.

292 [3] A. Shishlo et al., EPICS based virtual accelerator – concept and implementation, in:

293 Proceedings of Particle Accelerator Conference (PAC03), Portland, Oregon, 12–16 May 2003, p.
294 2366.

295 [4] J. Galambos et al., XAL application programming structure, In the Proceedings of Particle
296 Accelerator Conference (PAC05), Knoxville, Tennessee, 16–20 May 2005, pp4173

297 [5] Accelerator Technical Design Report for High-Intensity Proton Accelerator Facility Project,
298 JAERI-Tech 2003-044 and KEK Report 2002-13, Mar 2003

299 [6] SAD home page, <http://acc-physics.kek.jp/SAD/sad.html>

300 [7] D.C. Carey and F.C. Iselin, A standard input language for particle beam and accelerator
301 computer program

302 [8] S. Wolfram, Mathematica: A system for Doing Mathematics by Computer, Second Edition,
303 Addison-Wesley Publishing Company, 1991

304 [9] K. Ohmi, K. Hirata and K. Oide, From the beam-envelope matrix to synchrotron-radiation
305 integrals, Phys.Rev.E49, 4474, 1994

306 [10] Why Tcl?, <http://sunscript.sun.com/tcltext.html>

307 [11] F. Zimmermann, Measurement and Correction of Accelerator Optics, in: SLAC-PUB-7844,
308 Jun 1998, pp89

309 [12] T. Toyama, KEK-PS, Accelerator Study Note- 443, 2001, in Japanese

310 [13] I. Sakai, S. Machida, F. Noda and Y. Irie et al., H- Painting Injection System For The
311 J-PARC 3-GeV High Intensity Proton Synchrotron, In the Proceedings of Particle Accelerator
312 Conference (PAC03), Portland, Oregon, 12-16 May 2003, pp1512

313 [14] H. Harada, to be reported with PhD thesis

314

315 *Figure Captions:*

316 Figure 1: Accelerator control system in the J-PARC RCS. The VA is configured in the EPICS
317 IOC in parallel with the RA. The OPI can also directly call the VA as the online model (dashed
318 line).

319 Figure 2: The spectrum for betatron tune measurement by the VA with chromatic correction and
320 chopping factor of 0.11

321 Figure 3: The frequency spectrum displayed in Operation Interface for the horizontal
322 betatron-tune measurement. The peaks, which are frequency of 4.224, 4.084 and 4.365 MHz,
323 correspond to the revolution frequency of 9th harmonic and lower and upper sidebands of the
324 betatron tune, respectively.

325 Figure 4: Frequency deviation $\Delta f/f$ versus fractional part of horizontal betatron tune ν_x in the VA
326 (top) and RA (bottom)

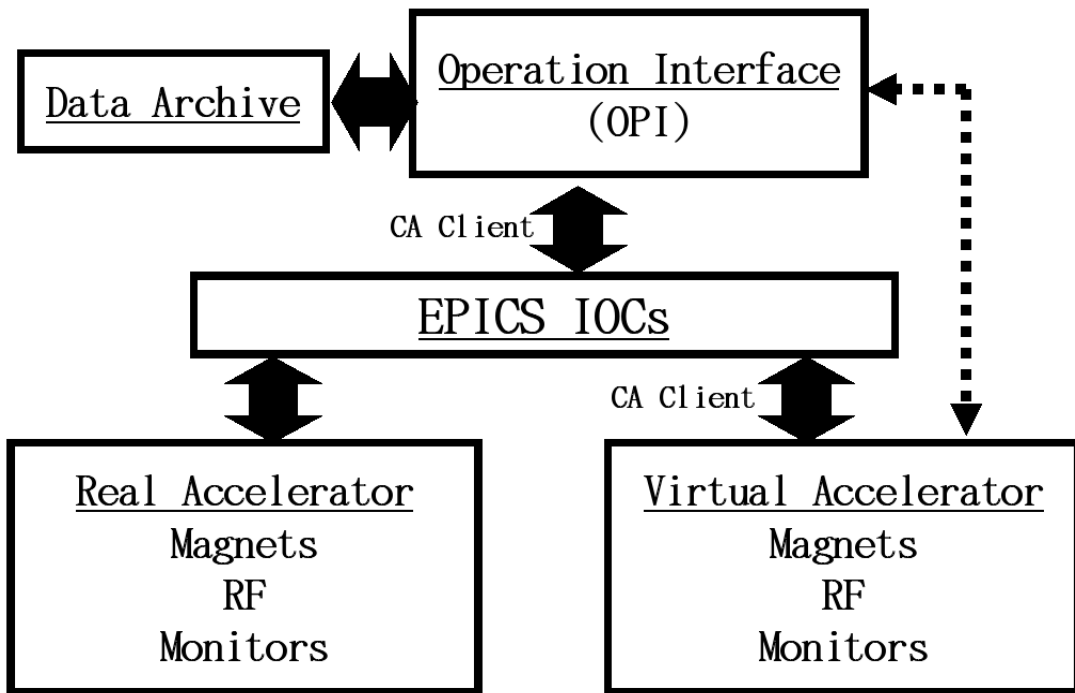
327 Figure 5: Layout of the RCS injection to dump line

328 Figure 6: Distribution of magnetic field for SBs. Red points show the measured magnetic field.
329 Rectangles show the regions of magnets; lines, the locations of foils and MWPMs.

330 Figure 7: Optics parameters before (top) and after (bottom) corrections in one super period of the
331 RCS. Beta function β_x for horizontal direction is plotted at the first trace; beta function β_y for
332 vertical direction is plotted at the second trace; dispersion function η_x for horizontal direction, at the

333 third trace. Solid lines are for design values; dots, for measured values at BPMs; and dashed line, for
334 the VA calculations.

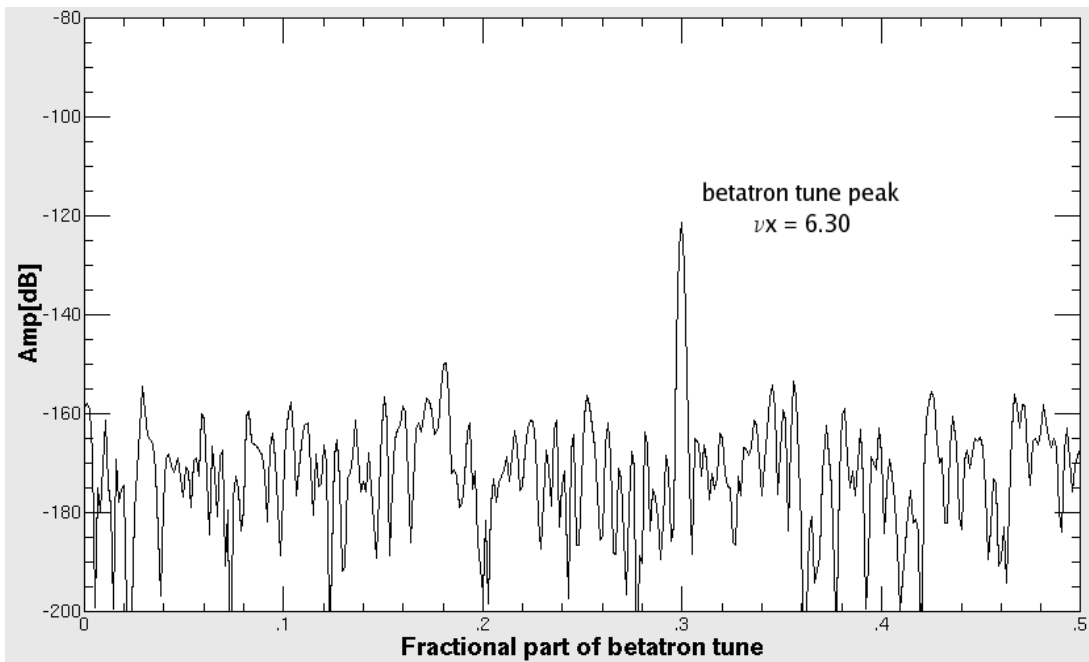
335 **Fig 1**



336

337

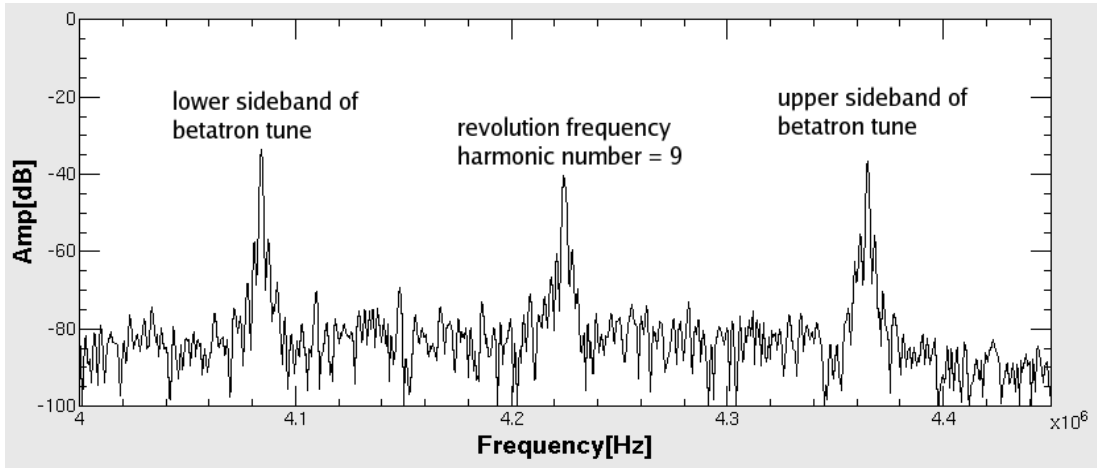
338 **Fig 2**



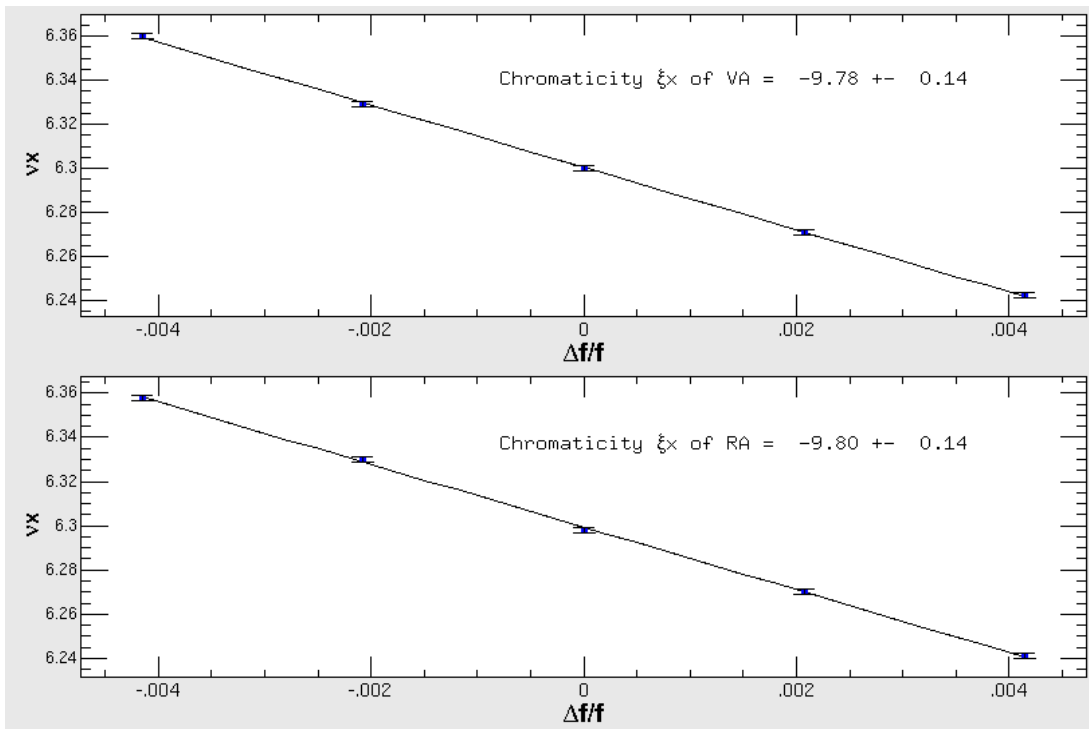
339

340

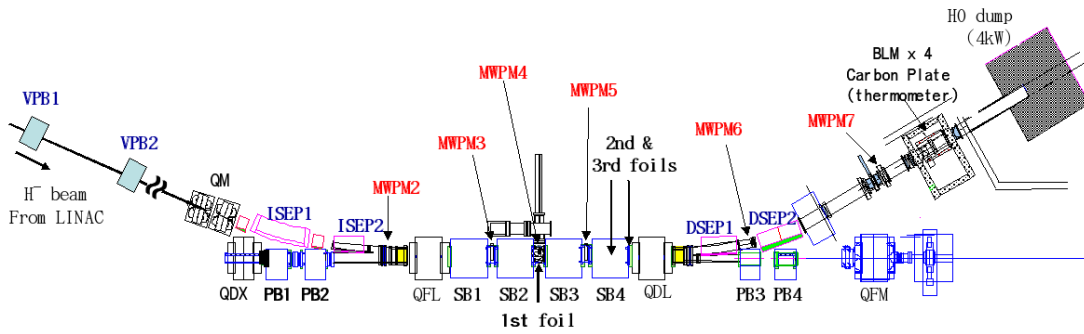
341 **Fig 3**



344 **Fig 4**



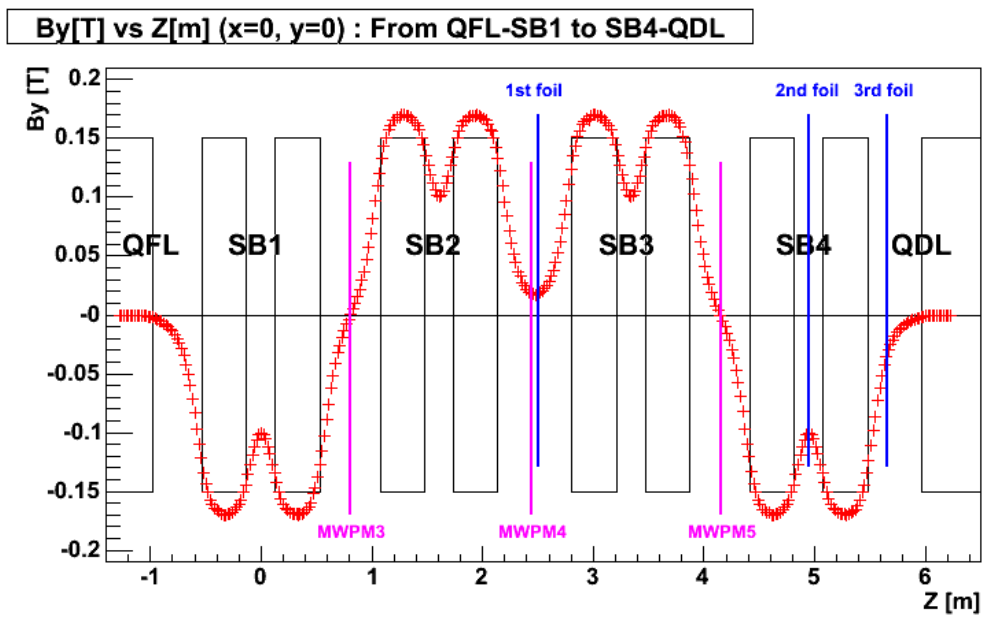
348 **Fig 5**



349

350

351 **Fig 6**



352

Fig7

